The Saudi Dental Journal 36 (2024) 1128–1134

Contents lists available at ScienceDirect

The Saudi Dental Journal

journal homepage: www.ksu.edu.sa
www.sciencedirect.com

Original Article

Enhancing orthodontic treatment control with fish scale-derived hydroxyapatite nanoparticles: Insights from an animal model study

Harraa S. Mohammed-Salih [a,*], Ataa Ghazi [b], Rana I. Mahmood [c], Haider H. Al-Qazzaz [d], Faridah Lisa Supian [e], Jameel R. Al-Obaidi [f,g,*], Majid Jabir [h]

[a] Department of Orthodontics, College of Dentistry, University of Baghdad, Baghdad 10047, Iraq
[b] P.O.P. Department, College of Dentistry, Mustansiriya University, Baghdad 10052, Iraq
[c] Department of Biomedical Engineering, College of Engineering, Al-Nahrain University, Jadriya, Baghdad, Iraq
[d] Department of Pathology, Teaching Laboratories, Al Yarmouk Teaching Hospital, Baghdad 10017, Iraq
[e] Department of Physics, Faculty of Science and Mathematics, Universiti Pendidikan Sultan Idris, 35900, Tanjong Malim, Perak, Malaysia
[f] Department of Biology, Faculty of Science and Mathematics, Universiti Pendidikan Sultan Idris, 35900, Tanjong Malim, Perak, Malaysia
[g] Applied Science Research Center. Applied Science Private University, Amman, Jordan
[h] Department of Applied Sciences -University of Technology, Baghdad 10066, Iraq

ARTICLE INFO

Keywords:
Biowaste utilisation
Dental biomaterials
Tooth movement

ABSTRACT

Objectives: This study investigates the impact of injected fish-scale-derived hydroxyapatite nanoparticles (FsHA-NPs) on orthodontic tooth movement (OTM) and the width of the periodontal ligament (PDL) space.
Materials and Methods: Twenty-six Wistar rats underwent mesial orthodontic traction with a force of 50 g for 21 days. Following the application of the orthodontic appliance, the rats were randomly divided into two groups: a control group, which received a 0.3 μg saline injection, and the experimental FsHA group, which received 100 mg/0.3 ml of FsHA-NPs after thorough characterisation. Injections were administered immediately after appliance application and repeated at 7 and 14 days. Statistical analysis was conducted with a significance level of $P \leq 0.05$.
Result: The experimental group exhibited a significant reduction in OTM at 7-, 14-, and 21-day post-force application. Additionally, a reduction in PDL width was observed in the mesiocervical and disto-apical regions of the mesial and distal roots of the first molar.
Conclusion: FsHA-NPs derived from biowaste fish scales exhibit promising potential as biomaterials for enhancing control over OTM. This study underscores the viability, accessibility, and safety of FsHA-NPs as a locally injectable material for orthodontic applications.

1. Introduction

The mechanical anchoring system in orthodontics plays a pivotal role and necessitates careful planning before commencing active orthodontic treatment to mitigate unwanted tooth movement (Retrouvey and Kousaie, 2021). Despite considerable advancements in biological research proposing innovative approaches to inhibit tooth movement and enhance stability, there remains a critical gap in effective strategies to prevent such undesirable sequelae (Swidi et al., 2018). Hydroxyapatite (HA) stands out for its exceptional biocompatibility and serves as a fundamental component in numerous synthetic biomaterials (Alhasyimi et al., 2021). Extensive research has been conducted to evaluate the efficacy of HA and its potential as a promising biomaterial for tissue defect regeneration and tissue engineering (Haraguchi, 2015). Various methods for synthesizing HA nanoparticles (HA-NPs) have been explored, including precipitation, hydrothermal, sol–gel, and microwave techniques (Alhasyimi et al., 2018). These methods enable the extraction of HA nanoparticles (HA-NPs) from biological waste sources such as fish scales, cow bone, and eggshells (Alhasyimi et al., 2017).

This study aims to investigate the effects of naturally derived fish scale hydroxyapatite nanoparticles (FsHA-NPs) on orthodontic tooth movement (OTM) in rat molars. The hypotheses posited are that FsHA-NPs can influence the rate of OTM and potentially enhance the stability of dental structures during and after treatment.

Peer review under responsibility of King Saud University.
* Corresponding authors.
E-mail addresses: dr.harraa_sabah@codental.uobaghdad.edu.iq (H.S. Mohammed-Salih), jr_alobaidi@yahoo.com (J.R. Al-Obaidi).

https://doi.org/10.1016/j.sdentj.2024.06.007
Received 1 February 2024; Received in revised form 22 May 2024; Accepted 2 June 2024
Available online 4 June 2024

2. Materials and methods

2.1. Synthesis of fish scales nanoparticles

Tilapia fish scales, procured from a local market in Selangor, Malaysia, served as the fundamental material for the synthesis of FsHA-NPs in this investigation. Initially, the dried scales underwent mechanical pulverisation into fine particles using a grinding machine. Subsequently, the powdered scales underwent calcination in a high-temperature furnace, initially heated to 800 °C for two hours and subsequently increased to 1000 °C for an additional two hours. As described previously (Zainol et al., 2012), the fish ash underwent wet grinding using ball milling for 48 h.

2.2. Characterisation of fish scales nanoparticles

The characterisation of the nanoproducts involved several tests, including x-ray diffraction (XRD) using a PHILIPS® PANalytical X'pert M.P.D. X-ray diffractometer (Almelo, Netherlands), scanning electron microscopy (SEM) coupled with Energy Dispersive X-ray Analysis (EDX) using a JEOL® JSM-7200F instrument (Peabody, Massachusetts, U.S.A.), and transmission electron microscopy (TEM) using a Zeiss LEO 9121 AB-100KV model (Germany).

2.3. Assessment of cytotoxicity of fish scales nanoparticles

The cytotoxicity evaluation of FsHA-NPs employed the 3-(4,5-dimethylthiazol-2-yl)-2,5-diphenyltetrazolium bromide assay (MTT assay) conducted on 96-well plates. Initially, rat embryo fibroblast (REF) cells were cultivated in RPMI-1640 medium supplemented with 10 % fetal bovine serum, 100 units/mL penicillin, and 100 µg/mL streptomycin. The cell culture was maintained at 37 °C with medium renewal twice a week (Al-Rahim et al., 2022).

2.4. Application of orthodontic traction force

This experiment utilized Wistar rats aged 2 to 3 months at the Institute of Iraqi Centre for Cancer and Medical Genetic Research, Al-Mustanseriah University. Ethical approval for this study was obtained from the ethics committee of the College of Dentistry, University of Baghdad, under reference number 896 and project number 896424. The experimental procedures adhered to the Animal Research: Reporting of in Vivo Experiments (ARRIVE) guidelines (Percie du Sert et al., 2020). For each experimental session, rats were sedated via intramuscular injection of ketamine (Rotexmedica™, Germany) and xylazine (Rompun®, Germany) at dosages of 80–100 mg/kg and 10–12.5 mg/kg, respectively. Mesial traction force was applied to the rat's first molar according to a previously described method with some adjustments (Kaipatur et al., 2014) (Fig. 1). This setup ensured a constant 50 g mesial traction force, as measured by a pointed tip Dentaurum® CORBLX pressure gauge (Germany). The mesial traction was sustained for a period of 21 days, until reaching the experimental endpoint.

2.5. Randomisation and group allocation

A total of 26 rats, each weighing between 250–350 g, were housed and subjected to orthodontic force. Random allocation into two groups was performed by numbering the cages from 1 to 26 and designating odd and even numbers. The control group (N = 13) received 0.3 ml saline injections, while the experimental group (N = 13) received injections of 100 mg/0.3 ml FsHA-NPs. The injection procedure was conducted immediately after applying traction forces and repeated at 7 and 14 days. The injections were administered into the palatal mucosa between the first and second right maxillary molars. Six rats expired during the

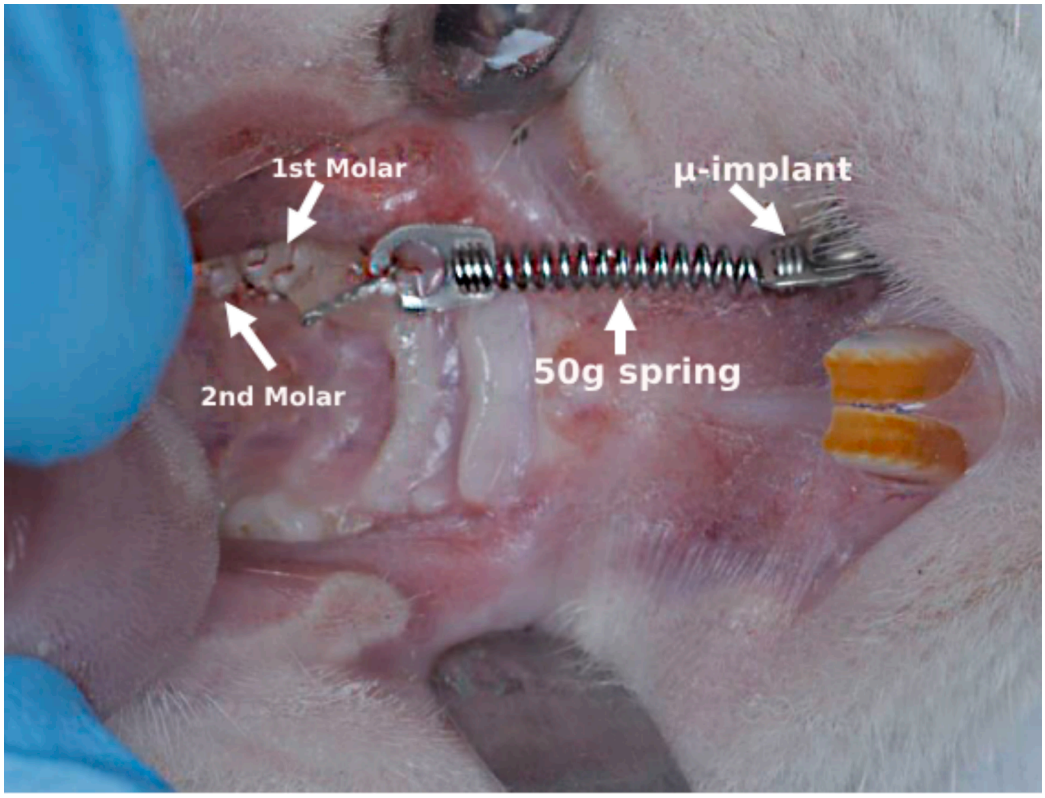

Fig. 1. The in-situ position of the experimental orthodontic appliance used to deliver a mesial traction force of 50 g to the rat's right 1st molar by a closed, short nickel-titanium coil spring (1 mm diameter, 0.2 mm thickness, 6 mm length; GAC International, Bohemia, New York, U.S.A.) which spanned from the right maxillary 1st molar to a self-drilled micro-implant (1.2 × 3 mm, Stryker-Leibinger Inc., Hamilton, Ontario, Canada) on the distopalatal side of the right maxillary incisor.

experiment, leaving 20 rats for further analysis.

2.6. Experimental measurements (Body weight and orthodontic tooth movement)

OTM was measured by taking vinyl polyether silicone impressions of the rats' upper dental arches under anaesthesia at 7-, 14-, and 21-day post-mesial traction. These impressions were digitized using a Medit® T710 desktop scanner (version 1.2.7, South Korea) and analyzed with exocad™ software (Darmstadt, Germany). The distance between two points in the most prominent area of the mesial marginal ridge of the second molar to that of the first molar, on both treated (right) and non-treated (left) sides, was calculated to quantify tooth movement (Fig. 2) (Pathomkulmai et al., 2022). The body weight of the animals was also monitored at specified intervals throughout the experiment to observe any physiological changes.

2.7. Histological measurement (Periodontal ligament width)

Animals were humanely sacrificed via an overdose injection of ketamine (Rotexmedica™, Germany) and xylazine (Rompun®, Germany), with every effort made to minimize pain. Following sacrifice, the maxillae were dissected and fixed in 10 % formalin for 48 h. Each paraffin specimen contained half of the maxilla with the three molars. Parasagittal sections parallel to the long axis of the first molar were cut at 5 μm and mounted on Leica Biosystems® Surgipath® Snowcoat® pearl microscope glass slides. These sections were then stained with Leica® haematoxylin and eosin (H&E) for histological analysis using an Olympus® light microscope (Japan) with objective lenses of 40 × and 100 × . The width of the periodontal ligament (PDL) was measured as previously described by Franzen et al. (Franzen et al., 2013), with measurements taken at the mesial and distal surfaces of the respective roots of the first molar. The areas M1 and M2 represented width measurements at the cervical and apical regions on the mesial surface, respectively, while D1 and D2 represented measurements on the distal surface, respectively (Supplementary data 1).

2.8. Statistical analysis

Data obtained for cytotoxicity were subjected to statistical analysis using an unpaired *t*-test with GraphPad® Prism 6. Results were expressed as mean (±) standard deviation (SD), derived from three independent measurements. Statistical evaluation was conducted using IBM® SPSS® version 22 (New York, U.S.A.). An intra-class correlation coefficients test was performed to assess the inter-examiner measurement reliability between two examiners, showing a good to excellent range of reliability. The normality distribution of numerical measures was assessed using the Shapiro–Wilk test. For each experimental setup across time and treatment groups, a one-way analysis of variance (ANOVA) was used to evaluate variation in normally distributed data on animal body weight and tooth movement. Furthermore, Šidák and Tukey post-hoc tests for multiple comparisons were employed to compare statistically significant test results across treatment groups and time-independent variables. Graphs were generated using GraphPad® Prism 8. The threshold for statistical significance was set at $P \leq 0.05$. Two-way ANOVA was conducted with a post hoc test (Tukey's multiple comparisons) to identify differences concerning the four variables across and within the groups.

3. Results

3.1. Characterisation of nanoparticles derived from fish scales

3.1.1. X-ray diffraction analysis

Upon analysis, FsHA-NPs exhibited three prominent peaks of significant intensity (Supplementary Data 2).

3.1.2. Scanning electron microscopy (SEM) and energy-dispersive X-ray (EDX) analysis

SEM examination of FsHA-NP revealed irregular size ranges and diverse shapes, ranging from cubes to hexagons (Fig. 3). EDX readings indicated the presence of Ca, O, P, and C phases within the FsHA-NPs (Supplementary Data 3).

3.1.3. Transmission electron microscopy (TEM) analysis

The histogram derived from TEM micrographs of FsHA-NPs depicted a particle size distribution range consistent with SEM, with a mean particle size of 57.7 nm (Supplementary Data 4A and B).

3.1.4. Cytotoxicity assays

Findings demonstrated good cell viability when comparing morphological changes in REF cells between the non-treated and FsHA-NP-treated groups (Supplementary Data 5).

3.2. Experimental measurements (Body weight and orthodontic tooth movement)

Šidák multiple comparison test results revealed no significant difference at 0- and 7-days post-appliance application. Surprisingly, at the last two time points (14 and 21 days), tooth movement was slower in the FsHA group compared to the control group (Table 1). Tukey multiple comparison tests between different time points showed significant

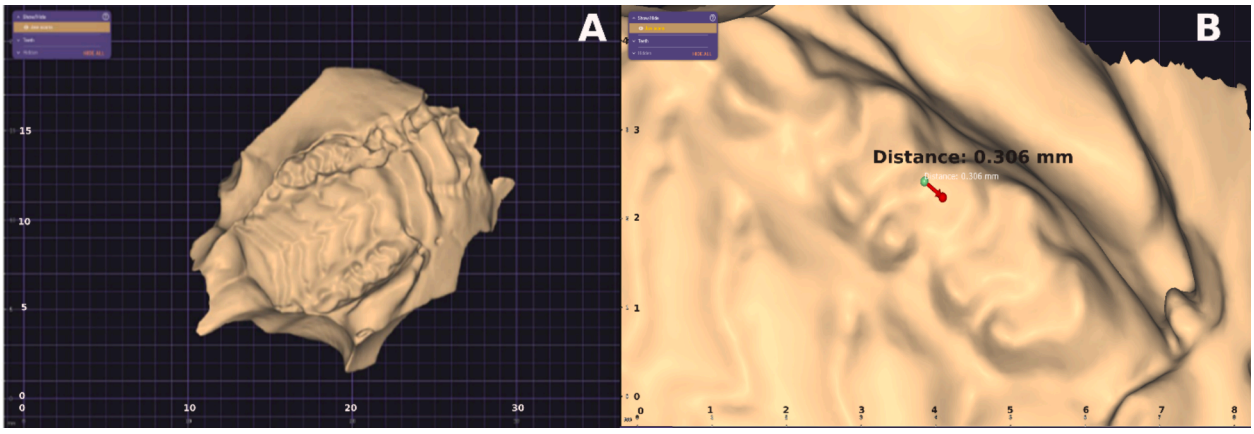

Fig. 2. The digital OTM measurement method. (A) The STL file was imported to exocad™ and (B) the amount of tooth movement was measured between two points on the proximal surfaces of the 1st and 2nd molar.

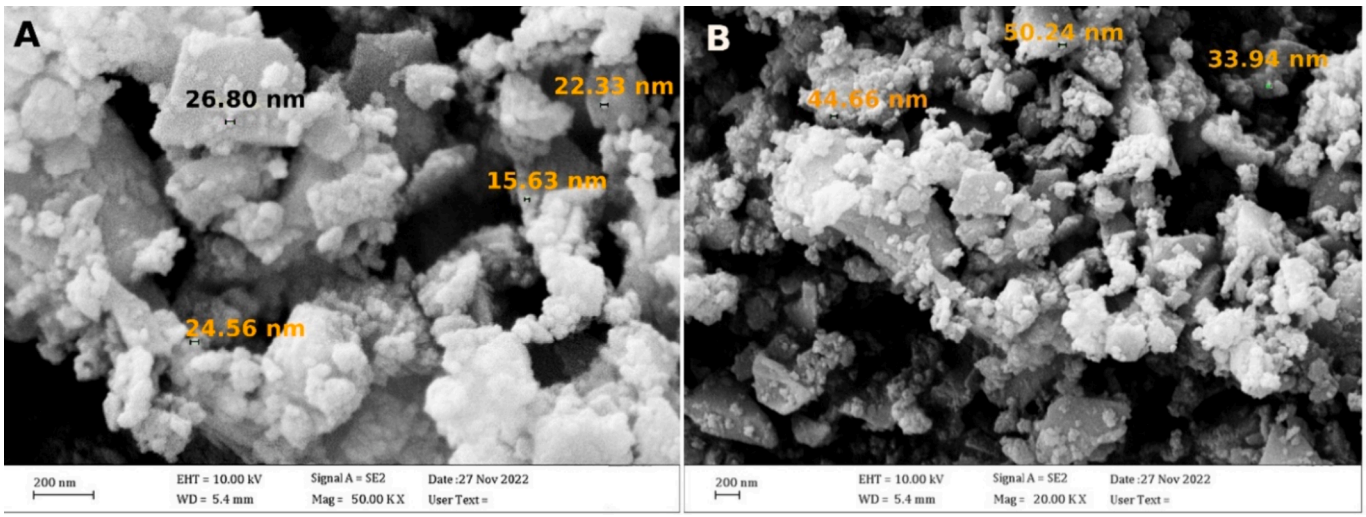

Fig. 3. SEM image depicting the particles' sizes of the FsHA-NPs ranging from (a) 22.33 nm to 26.80 nm and (b) 33.49 nm to 50.24 nm at the magnification of 20 K and 50 K.

Table 1
Šidák multiple comparisons test results of experimental OTM (mm) for studied groups at each time point.

Control – FsHA	Mean 1	Mean 2	Mean Diff.	95.00 % CI of diff.	Adjusted *P-value*
0	0	0	0	−0.06528 to 0.06528	> 0.9999
7	0.221	0.19	0.031	−0.03428 to 0.09628	0.6467
14	0.544	0.278	0.266	0.2007 to 0.3313	< 0.0001*
21	1.038	0.45	0.588	0.5227 to 0.6533	< 0.0001*

* Significant (*P-value* ≤ 0.05).

differences for each studied group, indicating slower tooth movement in the FsHA group across experimental intervals compared to the control group (Supplementary Data 6). Results in Table 2 underscored the significant influence of both time and treatment on experimental tooth movement.

Body weight measurements showed a significant decrease in both groups following force application, with no significant difference observed between the studied groups (Supplementary Data 7). The Šidák multiple comparison test revealed a significant decrease in the body weight of the animals post-orthodontic appliance, while the treatment factor showed no significant effect on body weight (Supplementary Data 8).

3.3. Periodontal ligament width

ANOVA and Tukey post-hoc analyses identified significant variations in PDL thickness across both FsHA and control groups, as well as among different locations within each group (Supplementary Data 9). Notably, within the FsHA group, PDL thickness at the M1 site was significantly greater (P-value < 0.05) than that observed at the M2 and D1 sites. In contrast, within the control group, PDL thickness at M1 was significantly lower (P-value < 0.05) than at M2 and D1 locations. Additionally, the M2 level was significantly higher than D1 locations within the control groups.

Between the groups, PDL thickness at the M1 location was significantly higher in the FsHA group compared to the control group, while the opposite was observed at the M2 level. At the D1 level, PDL width in the FsHA group was substantially below its counterpart in the control group, whereas at the D2 level of PDL, the FsHA group showed a significantly higher width compared to the control group (Supplementary Data 10). In Fig. 4, the micrograph of PDL space area illustrates the effect and interaction of injection on OTM along with a notable area of hypercementosis.

Table 2
Summary of Šidák multiple comparisons test results of experimental OTM (mm) across time and treatment factors.

Source of Variation	% of total variation	*P-value*
Interaction	13.25	<0.0001*
Time	72.22	<0.0001*
Treatment Factor	11.71	<0.0001*
Subjects (matching)	0.3701	0.9661

* Significant (*P-value* ≤ 0.05).

4. Discussion

This study synthesised FsHA nanoparticle powder from fish scales, with the nanoparticles characterised using XRD, SEM, and TEM. The XRD analysis confirmed the formation of standard HA indicating that the crystallite size is within the nanometric scale (Mudhafar et al., 2023), consistent with findings from other studies (Zhu et al., 2018). SEM analysis suggested that the FsHA-NP exhibits varying morphologies and some degree of agglomeration, likely due to static forces between particles, a finding corroborated by Majhooll et al. (Majhooll et al., 2019). TEM revealed poor dispersion and agglomerated particle morphology, comprising spherical particles and some nanorod-shaped apatite crystals. This aggregation behaviour can be attributed to the considerable surface area and energy of nanoparticles, in agreement with previous studies (Padmanabhan et al., 2009). Nanotechnology presents significant advancements and benefits in dentistry, with recent findings highlighting its potential, particularly in orthodontics. However, despite the recognized advantages of biowaste-derived nanomaterials, there remains a need for comprehensive validation of their risks and benefits (Zakrzewski et al., 2021; Mahmood et al., 2024).

According to the MTT assay results, FsHA-NP exhibited excellent cell viability and biocompatibility, suggesting its potential as a promising biomaterial for various biological applications (Sathiskumar et al., 2019). This study observed that the reduction in body weight of the animal post-application of orthodontic devices was consistent with previous experimental studies employing similar designs. Notably, the nanomaterial injection did not significantly impact the body weight of

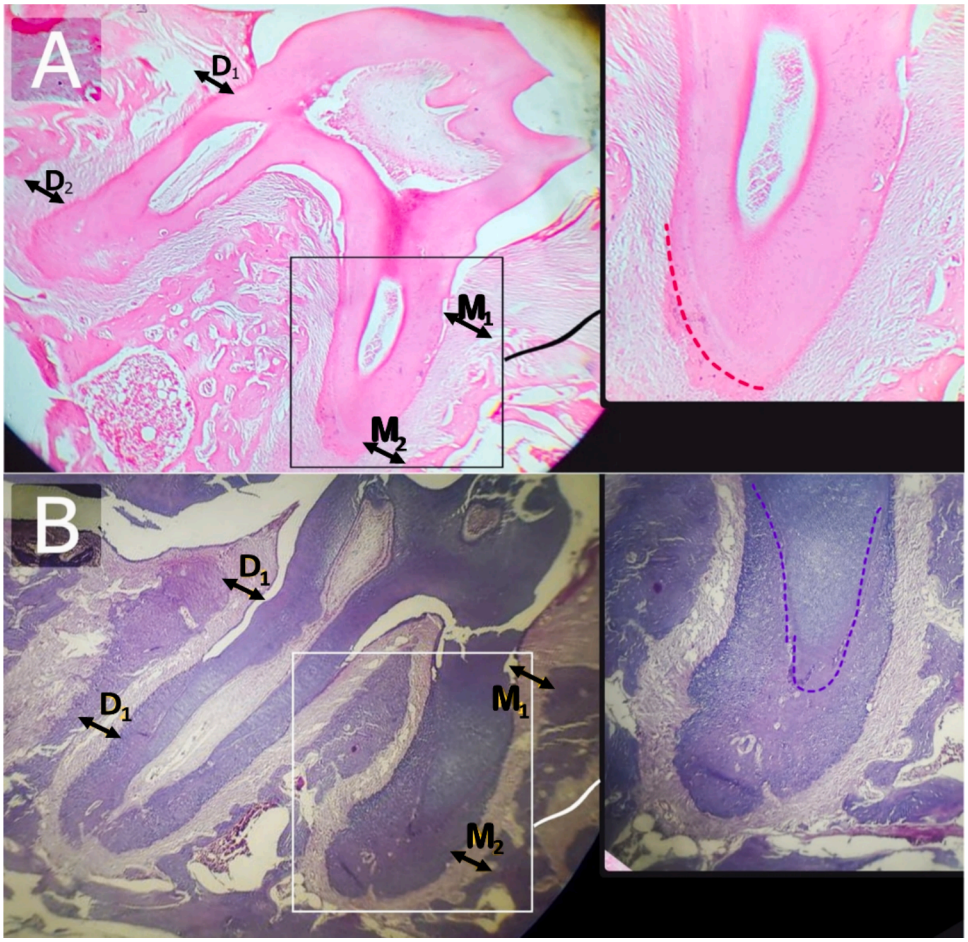

Fig. 4. The photomicrograph of the rats' 1st molar post orthodontic mesial traction showed histological changes in the periodontium. The PDL width of the (A) control group and the (B) FsHA group. The measurements were carried out at the cervical and apical region on both mesial (M1 and M2) and distal sides (D1 and D2), respectively (40X). Hypercementosis was observed in the apical region of the mesial root between the studied groups (100X).

the animal, as no significant difference was observed compared to the control group (Hara et al., 2015). While hydroxyapatite nanoparticles have been investigated for various applications (Refaat and Hamad, 2016; Malik and Ghaib, 2017; Khan et al., 2022), no prior studies have examined their local injection to assess the effects on OTM and PDL tissue. OTM is attributed to alveolar bone remodelling and PDL response to mechanical stimulation. Following mesial force application, the PDL space divides into compression and tension sites aligned with the force direction. This study found that the control group exhibited typical PDL responses. Conversely, the FsHA group demonstrated slower OTM after 14 days of force application, along with PDL widening at M1 and D2 sites, opposite the force direction. These findings are consistent with a previous study evaluating PDL width after mechanical retention on a rat molar (Franzen et al., 2013).

Studying PDL width in conjunction with OTM is crucial as it adheres to both new cementum and alveolar bone. Prior research has enhanced our understanding of periodontal fibroblastic cells' involvement in repairing bone defects when exposed to HA powder (Alhasyimi et al., 2018). A subpopulation of fibroblastic cells appeared to adapt to the presence of HA, exhibiting behaviour similar to osteoblastic cells under comparable conditions. It was found that nano-sized particles significantly enhance cell proliferation by increasing alkaline phosphatase activity after ten days of incubation compared to dense HA. Additionally, nano-sized HA accelerates osteogenic differentiation (Sun et al., 2007). Controlling unwanted tooth movement (precisely controlled anchorage) in orthodontics may be achieved through biological techniques influencing tooth movement at the molecular and cellular levels (Crawford et al., 2022). The results of this study suggest that FsHA-NP, a biocompatible and accessible biomaterial derived from biowaste, could serve as an effective biological orthodontic retainer. Local injection of FsHA-NP could help manage unwanted tooth movement by reinforcing the anchorage system in orthodontic treatments.

Since nano-hydroxyapatite exhibits significant osteoinductive potential and enhances osteointegration at the bone-implant interface, it has been extensively employed and studied in recent years. A recent study assessed the potential adhesion of PDL cells to a scaffold filled with HA particles derived from eggshells. The researchers observed improvements in the structural characteristics and sustained fibre viability of scaffolds (Espitia-Quiroz et al., 2022). However, a limitation of this study was that cellular and molecular interactions were not evaluated. Nonetheless, the clinical and histological findings corroborated previous in vitro studies examining PDL and bone tissue at cellular and molecular levels. Another recent study evaluated the effectiveness of naturally derived HA from *Portunus pelagicus* biowaste on bone defects. The researchers found that this material significantly enhanced the expression of bone morphogenetic protein-2 and inhibited the production of the proinflammatory cytokine interleukin-1, indicating the efficacy of the material in promoting periodontal tissue regeneration (Gani et al., 2022). The response of roots to OTM following force application has been studied at cellular and molecular levels, including the pathways of either resorption or formation (Mohammed-Salih et al., 2023). Recent research has focused on evaluating molecular events around the root area in response to force application via biochemical analysis of gingival crevicular fluid (Mohammed-Salih and Saloom, 2022). However, a

limitation of the current study was the collection of this fluid, as the minute size of the sulcus rendered its collection nearly impractical.

In this study, photomicrographs of the molars of rats treated with FsHA showed a remarkable area of hypercementosis around the apical part of the mesial root compared to the control group. The local injection of FsHA nanoparticles could trigger a cascade of molecular interactions, as functional groups of FsHA nanoparticles may conjugate with cementoblast-like cell receptors, leading to root hypercementosis (new cementum-like tissue formation) and increased alkaline phosphatase activity. A recent study demonstrated the expression of various genes and proteins when a composite of HA was applied to a culture of human PDL cells in vitro. The in vivo experiments indicated successful induction of cementum-like tissue formation, highlighting its osteogenic and cementogenic effects (Liao et al., 2020). These cementum reaction products could serve as promising conductive biomaterials for treating orthodontically induced inflammatory root resorption.

5. Conclusion

FsHA nanoparticles demonstrate potential as a cost-effective and safe material for clinically controlling undesired tooth movement. Our study observed unusual changes in the width of the PDL space following the application of orthodontic force in the experimental group. These changes may be associated with a significant reduction in OTM and the presence of hypercementosis near the apical region of the right first molar. The applicability of this research is limited by its reliance on an animal model, necessitating further research to confirm these findings in humans. Moreover, the long-term effects of FsHA nanoparticle injections require further investigation.

Ethical approval

This study was ethically approved by the ethics committee of the College of Dentistry, University of Baghdad (No. 3985 on 04 February 2023) and followed Animal Research: Reporting of in Vivo Experiments (ARRIVE) guidelines for experimental studies.

CRediT authorship contribution statement

Harraa S. Mohammed-Salih: Conceptualisation, Methodology, Writing – review & editing, Supervision. **Ataa Ghazi:** Validation, Investigation, Formal analysis, Project administration, Writing – original draft. **Rana I. Mahmood:** Validation, Investigation, Formal analysis, Project administration, Writing – original draft. **Haider H. Al-Qazzaz:** Data curation. **Faridah Lisa Supian:** Validation, Investigation. **Jameel R. Al-Obaidi:** Writing – original draft, Investigation. **Majid Jabir:** Data curation.

Declaration of competing interest

The authors declare that they have no known competing financial interests or personal relationships that could have appeared to influence the work reported in this paper.

Appendix A. Supplementary material

Supplementary data to this article can be found online at https://doi.org/10.1016/j.sdentj.2024.06.007.

References

Alhasyimi, A.A., Pudyani, P.S., Asmara, W., et al., 2017. Locally inhibition of orthodontic relapse by injection of carbonated hydroxy apatite-advanced platelet rich fibrin in a rabbit model. Key Eng. Mater. 758, 255–263. https://doi.org/10.4028/www.scientific.net/KEM.758.255.

Alhasyimi, A., Pudyani, P., Asmara, W., et al., 2018. Enhancement of post-orthodontic tooth stability by carbonated hydroxyapatite-incorporated advanced platelet-rich fibrin in rabbits. Orthod. Craniofac. Res. 21, 112–118. https://doi.org/10.1111/ocr.12224.

Alhasyimi, A.A., Suparwitri, S., Christnawati, C., 2021. Effect of carbonate apatite hydrogel-advanced platelet-rich fibrin injection on osteoblastogenesis during orthodontic relapse in rabbits. Eur. J. Dent. 15, 412–419. https://doi.org/10.1055/s-0040-1721234.

Al-Rahim, A.M., Mahmood, R.I., Mohammed, M.M., et al., 2022. In vitro evaluation of antioxidant and cytotoxic activity of folate-methotrexate conjugated to bovine serum albumin nanoparticles against MCF-7, HepG2, and PC3 cell lines. Gene Rep. 29, 101666 https://doi.org/10.1016/j.genrep.2022.101666.

Crawford, D., Lau, T.C., Frost, M.C., et al., 2022. Control of orthodontic tooth movement by nitric oxide releasing nanoparticles in Sprague-Dawley rats. Front. Mater. Sci. 9, 811251 https://doi.org/10.3389/fmats.2022.811251.

Espitia-Quiroz, L.C., Fernández-Orjuela, A.L., Anaya-Sampayo, L.M., et al., 2022. Viability and adhesion of periodontal ligament fibroblasts on a hydroxyapatite Scaffold combined with collagen, polylactic acid-polyglycolic acid copolymer and platelet-rich fibrin: A preclinical pilot study. Dent. J. 10, 167. https://doi.org/10.3390/dj10090167.

Franzen, T.J., Brudvik, P., Vandevska-Radunovic, V., 2013. Periodontal tissue reaction during orthodontic relapse in rat molars. Eur. J. Orthod. 35, 152–159. https://doi.org/10.1093/ejo/cjr127.

Gani, A., Yulianty, R., Supiaty, S., et al., 2022. Effectiveness of combination of chitosan gel and hydroxyapatite from crabs shells (Portunus pelagicus) waste as bonegraft on periodontal network regeneration through IL-1 and BMP-2 analysis. Int. J. Biomater. 2022 https://doi.org/10.1155/2022/1817236.

Hara, A. T., J. C. Carvalho and D. T. Zero, 2015. Causes of dental erosion: extrinsic factors. Dental Erosion and Its Clinical Management. B. T. Amaechi: 69-96.

Haraguchi, K., 2015. Application of CL/P Nanocomposites. Encyclopedia of Polymeric Nanomaterials. S. Kobayashi and K. Müllen. Berlin, Heidelberg, Springer Berlin Heidelberg: 49-57.

Kaipatur, N., Wu, Y., Adeeb, S., et al., 2014. A novel rat model of orthodontic tooth movement using temporary skeletal anchorage devices: 3D finite element analysis and in vivo validation. Int. J. Dent. 2014 https://doi.org/10.1155/2014/917535.

Khan, A.S., Alshaia, A., AlDubayan, A., et al., 2022. Preparation of nano-apatite grafted glass-fiber-reinforced composites for orthodontic application: Mechanical and in vitro biofilm analysis. Materials 15, 3504. https://doi.org/10.3390/ma15103504.

Liao, Y., Li, H., Shu, R., et al., 2020. Mesoporous hydroxyapatite/chitosan loaded with recombinant-human amelogenin could enhance antibacterial effect and promote periodontal regeneration. Front. Cell. Infect. Microbiol. 10, 180. https://doi.org/10.3389/fcimb.2020.00180.

Mahmood, R. I., H. S. Mohammed-Salih, A. a. Ghazi, et al., 2024. Exploring the potential of copper oxide biogenic synthesis: a review article on the biomedical and dental implementations. Arab Gulf J. Sci. Res. 42, 370-387. Doi: 10.1108/AGJSR-12-2022-0315.

Majhooll, A.A., Zainol, I., Jaafar, C.N.A., et al., 2019. Preparation of fish scales hydroxyapatite (FsHAp) for potential use as fillers in polymer. J. Chem. Chem. Eng. 13, 97–104. https://doi.org/10.17265/1934-7375/2019.03.002.

Malik, S.S.S., Ghaib, N.H., 2017. The effect of nano-hydroxy apatite on re-mineralize white spot lesions prior to orthodontic adhesive removal by different techniques (An In vitro comparative study). J. Baghdad College Dent. 29, 90–96. https://doi.org/10.12816/0038756.

Mohammed-Salih, H. S., H. A. Al-Lami, H. F. Saloom, et al., 2023. Detection of orthodontically induced inflammatory root resorption-associated biomarkers from the gingival crevicular fluid by proteomics analysis: a randomized-controlled clinical trial. 3 Biotech. 13, 157. Doi: 10.1007/s13205-023-03572-5.

Mohammed-Salih, H.S., Saloom, H.F., 2022. Collection, storage and protein extraction method of gingival crevicular fluid for proteomic analysis. Baghdad Sci. J. 19, 0368. https://doi.org/10.21123/bsj.2022.19.2.0368.

Mudhafar, M., Zainol, I., Alsailawi, H., et al., 2023. Preparation and characterization of FsHA/FsCol beads: Cell attachment and cytotoxicity studies. Heliyon 9. https://doi.org/10.1016/j.heliyon.2023.e15838.

Padmanabhan, S.K., Balakrishnan, A., Chu, M.-C., et al., 2009. Sol–gel synthesis and characterization of hydroxyapatite nanorods. Particuology 7, 466–470. https://doi.org/10.1016/j.partic.2009.06.008.

Pathomkulmai, T., Chanmanee, P., Samruajbenjakun, B., 2022. Effect of extending corticotomy depth to trabecular bone on accelerating orthodontic tooth movement in rats. Dent. J. 10, 158. https://doi.org/10.3390/dj10090158.

Percie du Sert, N., Hurst, V., Ahluwalia, A., et al., 2020. The ARRIVE guidelines 2.0: Updated guidelines for reporting animal research. J. Cereb. Blood Flow Metab. 40, 1769–1777. https://doi.org/10.1177/0271678X20943823.

Refaat, M.M., Hamad, T.I., 2016. Evaluation of mechanical and histological significance of nano hydroxyapatite and nano zirconium oxide coating on the osseointegration of CP Ti implants. J. Baghdad College Dent. 28 https://doi.org/10.12816/0031105.

Retrouvey, J.-M. and K. Kousaie, 2021. Basic Mechanics Applied to Orthodontics, International Foundation for Dental Education.

Sathiskumar, S., Vanaraj, S., Sabarinathan, D., et al., 2019. Green synthesis of biocompatible nanostructured hydroxyapatite from *Cirrhinus mrigala* fish scale–A biowaste to biomaterial. Ceram. Int. 45, 7804–7810. https://doi.org/10.1016/j.ceramint.2019.01.086.

Sun, W., Chu, C., Wang, J., et al., 2007. Comparison of periodontal ligament cells responses to dense and nanophase hydroxyapatite. J. Mater. Sci. Mater. Med. 18, 677–683. https://doi.org/10.1007/s10856-006-0019-8.

Swidi, A.J., Taylor, R.W., Tadlock, L.P., et al., 2018. Recent advances in orthodontic retention methods: A review article. J. World Fed. Orthod. 7, 6–12. https://doi.org/10.1016/j.ejwf.2018.01.002.

Zainol, I., Alwi, N., Abidin, M., et al., 2012. Physicochemical properties of hydroxyapatite extracted from fish scales. Adv. Mater. Res. 545, 235–239. https://doi.org/10.4028/www.scientific.net/AMR.545.235.

Zakrzewski, W., Dobrzynski, M., Dobrzynski, W., et al., 2021. Nanomaterials application in orthodontics. Nanomaterials 11, 337. https://doi.org/10.3390/nano11020337.

Zhu, Y., Xu, L., Liu, C., et al., 2018. Nucleation and growth of hydroxyapatite nanocrystals by hydrothermal method. AIP Adv. 8 https://doi.org/10.1063/1.5034441.